Effect of amplitude of walls on thermal and hydrodynamic characteristics of laminar flow through an asymmetric wavy channel

Article *in* Case Studies in Thermal Engineering · January 2022

DOI: 10.1016/j.csite.2022.101796

3 authors:

Sumit Kumar Mehta
National Institute of Technology, Silchar

Sukumar Pati
National Institute of Technology, Silchar

Laszlo Baranyi
University of Miskolc

Case Studies in Thermal Engineering 31 (2022) 101796

Contents lists available at ScienceDirect

Case Studies in Thermal Engineering

journal homepage: www.elsevier.com/locate/csite

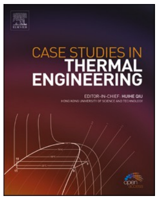

Effect of amplitude of walls on thermal and hydrodynamic characteristics of laminar flow through an asymmetric wavy channel

Sumit Kumar Mehta [a], Sukumar Pati [a], László Baranyi [b,*]

[a] Department of Mechanical Engineering, National Institute of Technology Silchar, Silchar, 788010, India
[b] Department of Fluid and Heat Engineering, Institute of Energy Engineering and Chemical Machinery, University of Miskolc, 3515, Miskolc-Egyetemváros, Hungary

HIGHLIGHTS

- Effects of *Re* and wall amplitude *A* studied for forced convective flow in a wavy channel.
- Linearly increasing (LIAC), decreasing (LDAC), constant amplitude (CAC) channels used.
- For higher *Re*, average *Nu* is highest for LIAC, followed by LDAC, then CAC.
- Performance parameter (*PF*) used to assess heat transfer and pumping power.
- For lower *Re* CAC has highest *PF*; for higher *Re*, *PF* is strongly dependent on *A*.

ARTICLE INFO

Keywords:
Wavy channel
Nusselt number
Performance factor
Forced convection

ABSTRACT

In this work, we investigate the hydrothermal characteristics for laminar forced convective flow of water through sinusoidal asymmetric wavy channel of three types: linearly increasing amplitude channel (LIAC), linearly decreasing amplitude channel (LDAC) and constant amplitude channel (CAC). The computed velocity and temperature fields are analyzed by varying the Reynolds number (*Re*) and slope (*A*) of the linearly varying amplitude in the following ranges: $5 \leq Re \leq 200$ and $0.02 \leq A \leq 0.04$. The value of average Nusselt number is almost independent on the geometry of the channel at lower values of *Re* and *A*. At higher *Re* values, the average Nusselt number is the highest for LIAC followed by LDAC, and CAC. The combined effects of heat transfer increase in the wavy channel compared to plane channel and the associated pumping power is assessed using performance parameter (*PF*). For lower *Re* values the highest *PF* is obtained for CAC. For higher values of *Re* the *PF* is the largest for LDAC at $A = 0.02$ and 0.03, and the value of *PF* for $A = 0.04$ is the highest for CAC.

Nomenclature

A	slope of the linearly varying amplitude (-)
c_p	specific heat of the fluid (J kg^{-1}K^{-1})
ER	enhancement ratio (-)
k	thermal conductivity (W m^{-1} K^{-1})

* Corresponding author.
E-mail addresses: sukumar@mech.nits.ac.in (S. Pati), laszlo.baranyi@uni-miskolc.hu (L. Baranyi).

https://doi.org/10.1016/j.csite.2022.101796
Received 21 November 2021; Received in revised form 10 January 2022; Accepted 12 January 2022
Available online 20 January 2022

L	inlet half height of the channel (m)
Nu	local Nusselt number (-)
$\overline{Nu}$	average Nusselt number (-)
n	dimensionless outward normal to the wall (-)
p	pressure (Pa)
PF	performance factor (-)
PR	pressure ratio (-)
Re	Reynolds number (-)
$S(x)$	profile of the wavy wall (m)
T	temperature (K)
u, v	two-dimensional velocity components (m/s)
x, y	dimensional axial and transverse coordinates (m)

Greek symbols

θ	dimensionless temperature (-)
μ	dynamic viscosity (kg m^{-1} s^{-1})
ρ	density of the fluid (kg m^{-3})

Acronyms

CAC	Constant amplitude channel
LDAC	Linearly decreasing amplitude channel
LIAC	Linearly increasing amplitude channel

1. Introduction

The use of a wavy channel is one of the best methods of achieving heat transfer increase in various fields including solar and process plants, heat exchangers, and processes involving polymetric composite manufacturing [1]. Passive and active methods are used for heat transfer augmentation for any transport processes [2]. The active methods require external power in addition to the pumping power to maintain the enhancement mechanism, while passive techniques mostly consist of changing the surface area introducing waviness in the wall [3–6], using baffles [7,8], nanofluid [9–15], and porous media [9,16–18]. The dynamics of flow through a wavy channel becomes complicated even for laminar flow because of the formation of flow recirculation zones. Accordingly, a thorough understanding in the transport dynamics is of utmost importance in designing thermal systems involving corrugated channels.

A plethora of articles are available in the literature on laminar forced convection flow through corrugated channels, investigating the effect of corrugation geometry on the heat transfer enhancement with minimum pressure drop. Rush et al. [19] analyzed laminar forced convection in sinusoidal converging-diverging channel and found a local enhancement in heat transfer with Reynolds number *Re*. Wang and Chen [20] analyzed the effect of amplitude of the sinusoidal wall on heat transfer increase and frictional losses for laminar flow. Naphon [21–24] conducted a number of numerical and experimental works to analyze the forced convection hydro-thermal transport in corrugated channels. Akbarzadeh et al. [25] studied the thermo-hydraulic characteristics for laminar forced convection through three types of corrugated channels: triangular, trapezoidal, and sinusoidal. They found that at higher *Re* the corrugated channel is advantageous in terms of higher heat transfer rate. Rashidi et al. [26] numerically investigated the effect of geometrical parameters of the sinusoidal wavy channel on the thermo-hydraulic performance and total entropy generation for turbulent flow. Shubham et al. [27] analyzed the effect of fluid rheology on the thermo-hydraulic performance for laminar forced convection in wavy channel. Pati et al. [28] conducted a comparative assessment of the thermo-fluidic performance in two wavy channels for laminar forced convection. Ermagan and Rafee [29,30] investigated the effect of superhydrophobic wall on the thermo-hydraulic performance of wavy microchannel heat sink and suggested that lower amplitude and higher wavelength is suitable for better performance. Several works [31–38] analyzed the effect of geometrical parameters on the heat transfer augmentation in corrugated channels. Mehta and Pati [39] investigated the thermo-hydraulic performance for triangular corrugated channel in laminar regime. Alawadhi [40] analyzed the effect of linearly increasing amplitude in the entrance region of a sinusoidal wavy channel on the heat transfer and pressure drop for laminar forced convection and found that such type of channel is more effective for heat transfer at higher amplitude and lower Reynolds number. It has also been found that the increase in the entrance length of increasing amplitude decreases the pressure drop. Nandi and Chattopadhyay [41,42] investigated the heat transfer characteristics for the pulsating forced convective flow through a wavy microchannel in the laminar regime by varying the Reynolds number and Strouhal number. Tiwari and Moharana [43,44] studied the thermo-hydraulic performance for the conjugate heat transfer through the raccoon and wavy microchannel. They found that the performance of the raccoon microchannel is better than the wavy and plane microchannels. Recently a number of studies have been conducted to investigate the heat transfer characteristics for flow through wavy channels, including nanofluid [9,10,45–49], porous materials [9], magnetic field [10], and ribs [50].

Although there are several research articles in the literature analyzing the thermo-hydraulic performance for laminar flow in wavy channel, most of the works deal with channels with constant amplitude. The efficacy of the varying amplitude of the wall of wavy channel on the hydrothermal performance is not yet explored. Accordingly, a comprehensive numerical investigation is performed to

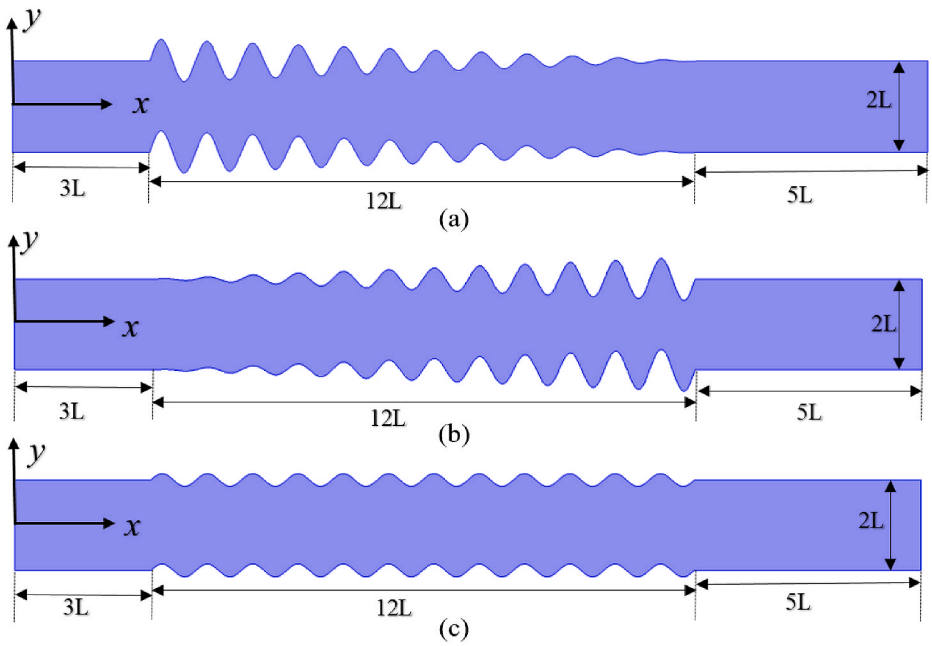

Fig. 1. Physical domain of the considered wavy channels: (a) linearly decreasing amplitude channel (LDAC), (b) linearly increasing amplitude channel (LIAC), and (d) constant amplitude channel (CAC).

assess the efficacy of the varying amplitude of the wall of wavy channel on the hydrothermal performance for laminar flow regime. A comparison on the hydrothermal performance is made for the linearly increasing- and decreasing amplitude channel with the constant amplitude wavy channel.

2. Theoretical formulation

Forced convective laminar flow of water (Prandtl number = 6.93) through one of three types of sinusoidal asymmetric wavy channels is considered as shown in Fig. 1(a)-(c): a linearly increasing amplitude channel (LIAC), a linearly decreasing amplitude channel (LDAC), and a constant amplitude channel (CAC). The phase difference of the top and bottom walls is 180°. The profiles of the top wall are as follows:

For LIAC:

$$S(x) = L + A(x - 3L)\sin(2\pi(x - 3L)/L). \tag{1}$$

For LDAC:

$$S(x) = L - A((x - 3L) - 12L)\sin(2\pi(x - 3L)/L). \tag{2}$$

For CAC:

$$S(x) = L + (A_m L)\sin(2\pi(x - 3L)/L), \tag{3}$$

where the linearly increasing and decreasing amplitudes are $A(x-3L)$ and $A((x - 3L) - 12L)$, respectively. The amplitude ($A_m L$) for the CAC is calculated by considering the same total flow passage area of the wavy part of the channel. The range of the slope of linearly varying amplitude A investigated is $0.02 \le A \le 0.04$. The lengths of the inlet and outlet adiabatic flat part are $3L$ and $5L$, respectively. The wavelength of the wavy channel is constant ($=L$). The length of the isothermal part of wavy walls is $12L$, as shown in Fig. 1. The parameter ranges are the same as in Refs. [3,20,39]. The internal heat generation and the radiation heat transfer are neglected. The steady flow of incompressible constant-property fluid is considered [3,20].

The governing transport equations are the conservation of mass, momentum, and energy; the corresponding mathematical forms are written as [3,20]:Continuity equation

$$\frac{\partial u}{\partial x} + \frac{\partial v}{\partial y} = 0, \tag{4}$$

x-momentum equation

$$\rho\left[u\frac{\partial u}{\partial x} + v\frac{\partial u}{\partial y}\right] = -\frac{\partial p}{\partial x} + \mu\left(\frac{\partial^2 u}{\partial x^2} + \frac{\partial^2 u}{\partial y^2}\right), \tag{5}$$

y-momentum equation

$$\rho\left[u\frac{\partial v}{\partial x}+v\frac{\partial v}{\partial y}\right]=-\frac{\partial p}{\partial y}+\mu\left(\frac{\partial^2 v}{\partial x^2}+\frac{\partial^2 v}{\partial y^2}\right), \tag{6}$$

Energy equation

$$u\frac{\partial T}{\partial x}+v\frac{\partial T}{\partial y}=\frac{k}{\rho c_p}\left[\frac{\partial^2 T}{\partial x^2}+\frac{\partial^2 T}{\partial y^2}\right]. \tag{7}$$

The boundary conditions are:
At inlet:

$$u=u_{inlet}, \tag{8a}$$

$$T=T_{inlet}=300\text{K}, \tag{8b}$$

On the walls:

$$u=v=0, \tag{9a}$$

$$\frac{\partial T}{\partial y}=0 \text{ for } x<3L,\ x>15L \tag{9b}$$

$$T=T_w=310\text{K for } 3L\le x\le 15L, \tag{9c}$$

At outlet:

$$p=p_{atm};\ \frac{\partial T}{\partial x}=0. \tag{10}$$

The local heat transfer is characterized by the local Nusselt number (Nu) defined as [3]:

$$Nu=-\frac{\partial\theta}{\partial n}. \tag{11}$$

Here n is the dimensionless unit outward normal, which is normalized by L, and θ is a dimensionless temperature [3]:

$$\theta=\frac{(T-T_{inlet})}{(T_w-T_{inlet})}. \tag{12}$$

The average Nusselt number is calculated as [3]:

$$\overline{Nu}=\frac{\int_{3L}^{15L} Nu\,\mathrm{d}S}{\int_{3L}^{15L}\mathrm{d}S}, \tag{13}$$

where S is the arc length along the wavy wall.

We introduce two parameters: the enhancement ratio (ER) and the pressure drop ratio (PR) to characterize the increment of heat transfer rate and the corresponding pressure drop in a wavy channel in comparison with an equivalent straight channel, [3]:

$$ER=\overline{Nu}_{wavy}\Big/\overline{Nu}_{plane}, \tag{14}$$

$$PR=\Delta p_{wavy}\big/\Delta p_{plane}. \tag{15}$$

The percentage enhancement in heat transfer in a wavy channel compared to that of plane channel is presented by the percentage enhancement (PE):

$$PE=\frac{\left(\overline{Nu}_{wavy}-\overline{Nu}_{plane}\right)}{\overline{Nu}_{plane}}\times 100. \tag{16}$$

The combined effects of heat transfer enhancement and the corresponding pressure drop penalty in wavy channel over an equivalent plane channel are characterized by the performance factor (PF) [39]:

$$PF=\frac{ER}{(PR)^{1/3}}, \tag{17}$$

Table 1
Grid independency test for a linearly decreasing amplitude channel (LDAC) at $Re = 100$.

A	No. of elements	$\overline{Nu}$	Relative difference (%)
0.02	12012	5.1123	10.38
	32031	4.9123	6.06
	61243	4.6638	0.70
	112345	4.6312	–
0.03	15213	5.5727	13.86
	41235	5.1529	5.28
	86095	4.9092	0.308
	134226	4.8941	–
0.04	18123	5.7688	12.20
	51234	5.2902	2.89
	91234	5.1465	0.103
	151223	5.1412	–

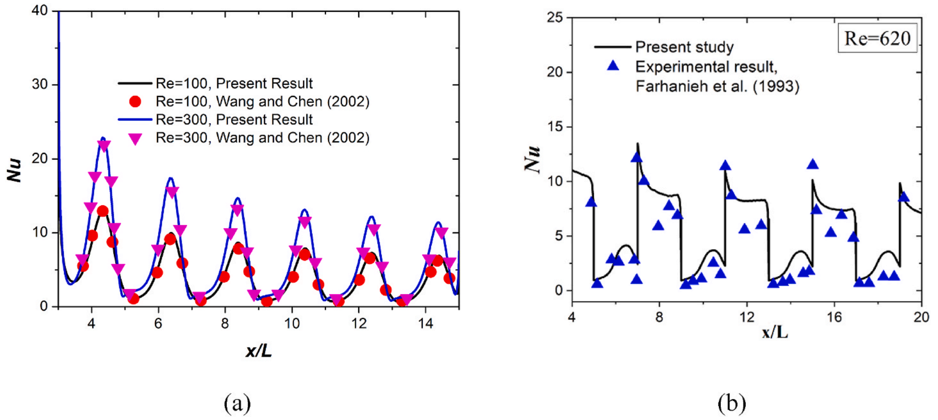

Fig. 2. (a) Comparison of Nu along the bottom wavy wall with the results of Wang and Chen [20] at $Re = 100$ and 300 and constant dimensionless amplitude of 0.2. (b) Comparison of Nu along a rectangular corrugated wall with the experimental results of Farhanieh et al. [51] for air flow through a rectangular-grooved duct at $Re = 620$.

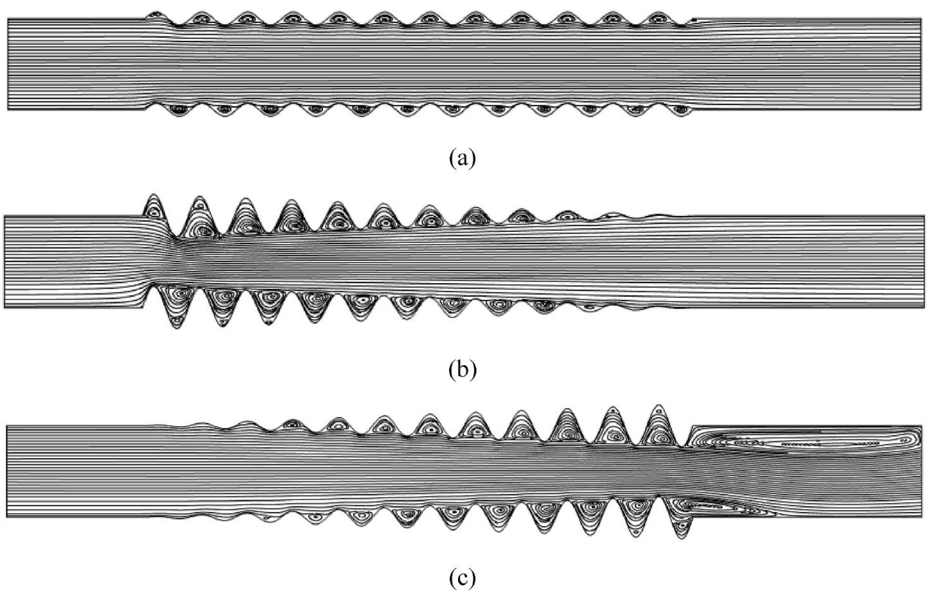

Fig. 3. Streamlines at $Re = 200$ and $A = 0.04$ for (a) CAC, (b) LDAC and (c) LIAC.

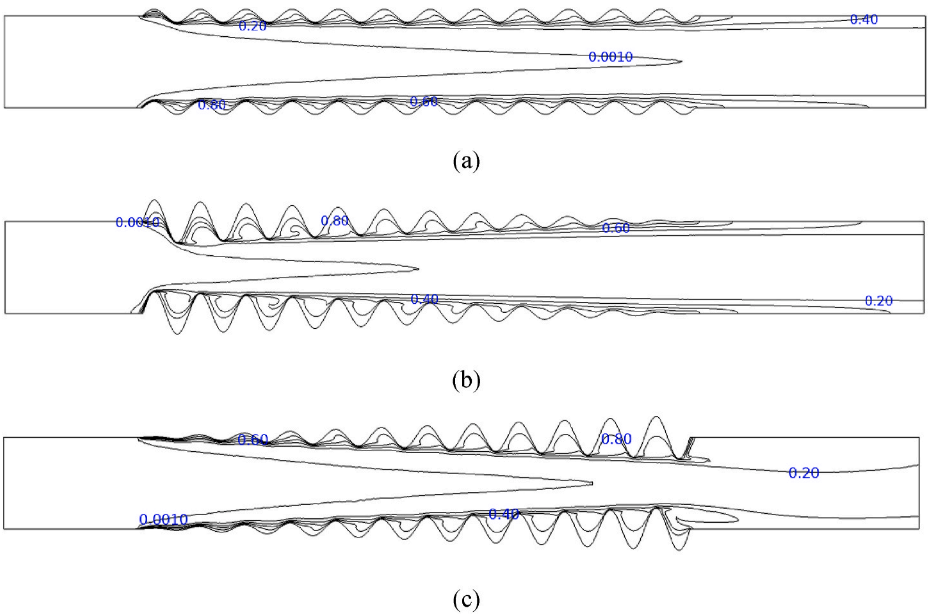

Fig. 4. Isotherms at $Re = 200$ and $A = 0.04$ for (a) CAC (b) LDAC and (c) LIAC.

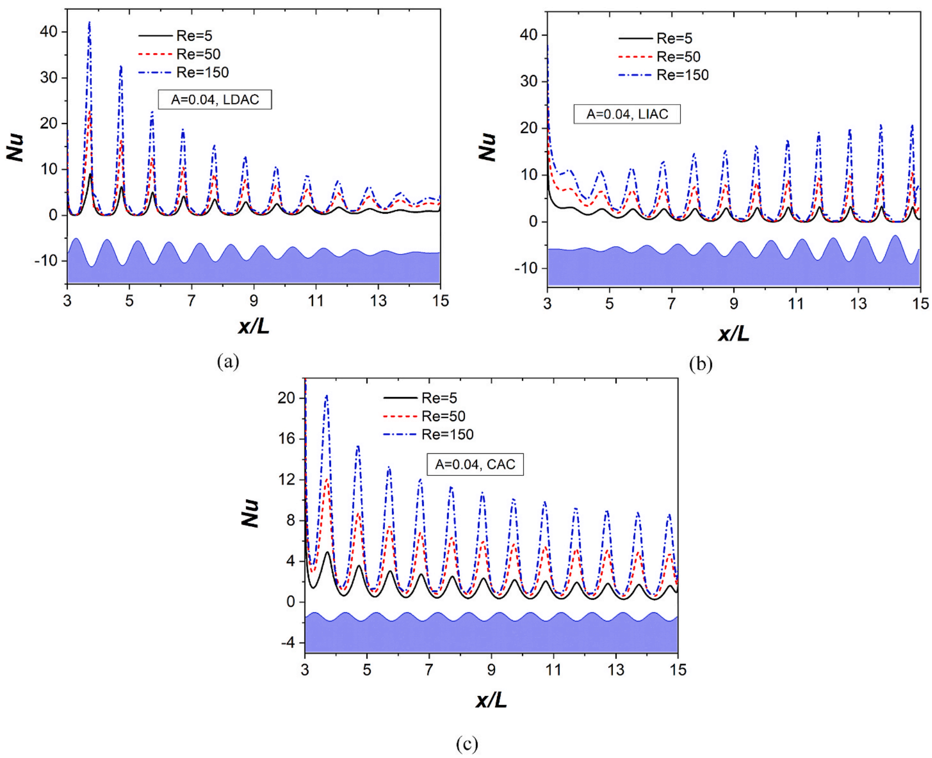

Fig. 5. Variation of *Nu* at the top wall with (a) LDAC (b) LIAC and (c) CAC for $A = 0.04$. The top half of the channels are shown in the insets.

3. Numerical method and validation

A finite element method based numerical solver is used to solve the governing transport equations with the boundary conditions. The mesh is non-uniform in the computational domain and dense near the boundary. The Galerkin weighted residual method is used for the discretization and system of equations obtained are solved by iteration until the convergence criteria $\max\left|\varphi^{n+1} - \varphi^{n}\right| / \varphi^{n} \leq 10^{-6}$ (φ is a transport variable) are satisfied. The grid independence test has been performed for all geometries, and the grids are finalized for

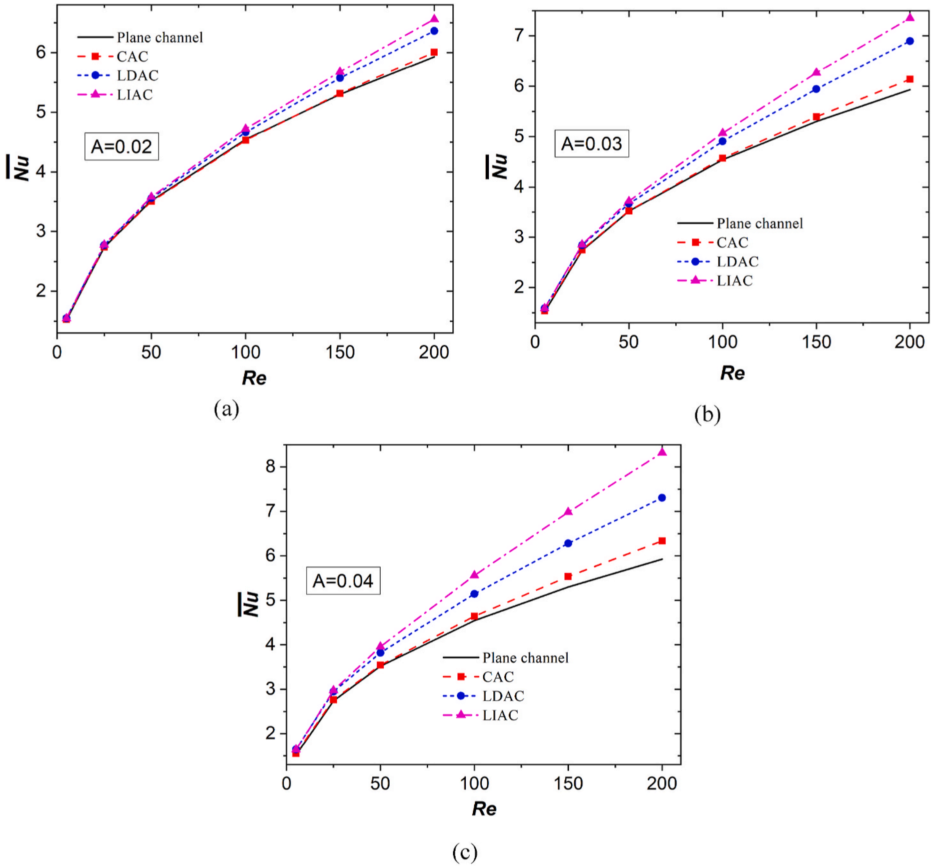

Fig. 6. Variation of $\overline{Nu}$ with Re at (a) A = 0.02, (b) A = 0.03 and (c) A = 0.04.

simulations such that the relative differences in $\overline{Nu}$ are less than 1% compared to a highly refined mesh. The results of the grid independency test for the linearly decreasing amplitude channel (LDAC) are shown in Table 1 at Re = 100.

We perform extensive validation prior to conduct the simulations. Firstly, the present model is validated with the numerical work of Wang and Chen [20] for laminar forced convection in wavy channel as shown in Fig. 2 (a). We perform another validation with the experimental results of Farhanieh et al. [51] for air flow through a rectangular-grooved duct as shown in Fig. 2(b). The two comparisons show a good agreement, thus confirming the accuracy of the solver.

4. Results and discussion

The objective of the present work is to analyze the hydrothermal characteristics for flow through a sinusoidal wavy channel of three different types: a linearly increasing amplitude channel (LIAC), a linearly decreasing amplitude channel (LDAC), and a constant amplitude channel (CAC). The temperature and flow fields are presented for the Reynolds number ($Re = (\rho u_{\text{inlet}} L)/\mu$) in the range of $5 \leq Re \leq 200$ [3]. The range of A is $0.02 \leq A \leq 004$, similar to the ranges in Refs. [3,20,27,28].

To study the involved flow physics for different types of wavy channels considered in this study, the streamlines are shown in Fig. 3 at A = 0.04 and Re = 200. The bulk flow decelerates in LDAC (Fig. 3(a)) due to increase of the effective cross-sectional area of the channel in the direction of the flow, leading to adverse pressure gradient, while for LIAC the bulk flow accelerates (Fig. 3(b)) resulting in favorable pressure gradient. Beyond a certain Re the flow is attached and detached alternately while flowing through the wavy passages in the channel because of the favorable pressure gradient in the converging passage (see Fig. 3(b)) and the adverse pressure gradient in the diverging passage (Fig. 3(c)). Beyond a critical value of Re the magnitude of positive pressure gradient in diverging conduits increases over the threshold value and the flow gets separated resulting in recirculation zones. At low Re (=5), no recirculation zone is formed for CAC, although recirculation zones are formed for LIAC and LDAC for the waves near the outlet and inlet, respectively. Moreover, additional recirculation zones are also formed even at lower Reynolds numbers for LIAC and LDAC in the inlet and outlet of the corrugated section, respectively.

The formation of the recirculation zone causes trapping of hot fluid, and the attachment of the primary flow causes higher velocity, as well as temperature gradient. To analyze the temperature field of different wavy channels, dimensionless isotherms are shown in Fig. 4. It can be seen in the figure that the core zone of the cold fluid for LDAC is shifted towards the upstream direction compared to LIAC. This is because of the larger size of recirculation zones in the upstream section for LDAC (see Fig. 3). The effective heat transfer

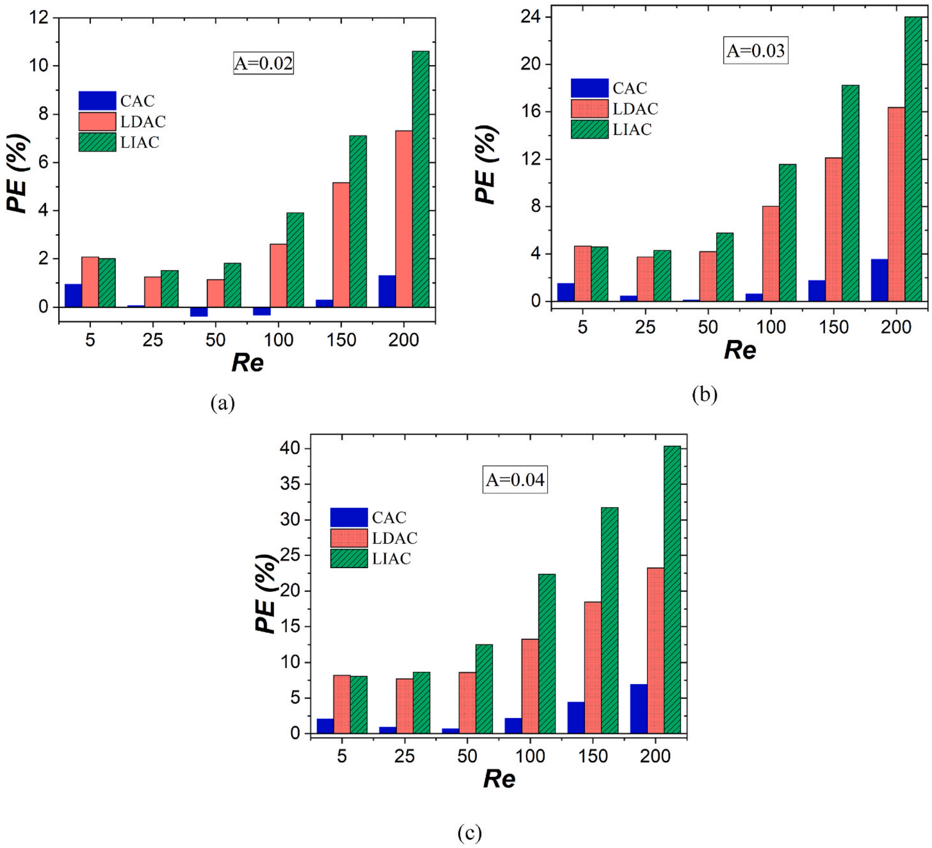

Fig. 7. Variation of percentage enhancement of heat transfer (*PE*) for different types of wavy channels at (a) $A = 0.02$, (b) $A = 0.03$ and (c) $A = 0.04$.

area in the entrance region is the highest for LDAC. Due to the trapping of fluid in the recirculation zones, the temperature of the fluid in this zone is relatively high and almost constant. Therefore, the higher values of isotherms occur away from the hot wall for the larger recirculation zone.

To investigate the effect of channel wall geometry on the local heat transfer rate, the variation of local Nusselt number *Nu* at different *Re* is shown for the three different wavy channels in Fig. 5. The *Nu* pattern mimics the channel geometry in a sense that there is a local maximum and a local minimum in each wave, and their magnitudes are strongly dependent on the wall topology. The values of maxima of local Nusselt number increase with *Re* because of the increased advection, although the minima values of *Nu* are almost independent of *Re*. This is because the trapping of the hot fluid at higher *Re* and velocity reduction at low *Re* leads to lower heat transfer rate. It can be seen that the value of the maxima of *Nu* is the highest for LDAC followed by LIAC and CAC. This is because of the combined effects of the higher velocity gradient near the entrance region and the lower bulk fluid temperature at the entrance region for LDAC.

Fig. 6 shows the combined effects of *Re* and amplitude *A* on the heat transfer (average Nusselt number ($\overline{Nu}$) against *Re*). It can be seen that average Nusselt number is almost independent of the channel geometry at lower *Re* and *A* values. However, with the increase in *Re* and *A* the effect of channel geometry grows. The average Nusselt number is always greater for the wavy channel than for the plane channel, even for CAC. The value of average Nusselt number is the highest for LIAC followed by LDAC and CAC. The higher amplitude of LIAC near the outlet results in a higher velocity as well as temperature gradients, thus enhancing the heat transfer. The temperature of the bulk fluid near the outlet is higher, and thus enhancement in heat transfer is somewhat smaller. It can be seen in Fig. 5 that the magnitude of the local maxima of *Nu* near the outlet for LIAC is smaller than the corresponding maxima near the inlet for LDAC. Similarly, the minimum value of local maxima of *Nu* near the inlet for LIAC is higher than the corresponding maxima value for LDAC near the outlet.

To investigate the efficacy of the wavy channel with respect to the heat transfer enhancement compared to a plane channel, the percentage enhancement in heat transfer (*PE*) is presented in Fig. 7 at different *Re*. The *PE* decreases with *Re* up to a critical value of Reynolds number (Re_{crit}) and thereafter increases in the investigated domain for all types of wavy channels. However, for $Re < Re_{crit}$ the decrement of *PE* with *Re* is smaller for higher values of *A*. At lower *Re* the advection is lower, hence the increment in *Nu* is relatively small in this zone. The recirculation region causes trapping of hot fluid and resists the heat transfer in the corresponding region. The combined effect causes an overall decrease in *PE* for lower *Re*. However, for higher values of *Re*, the increment of maxima values of *Nu* causes an increase in the *PE* value. The value of Re_{crit} varies with the channel geometry. For example, for CAC, $Re_{crit} = 50$ for all *A*

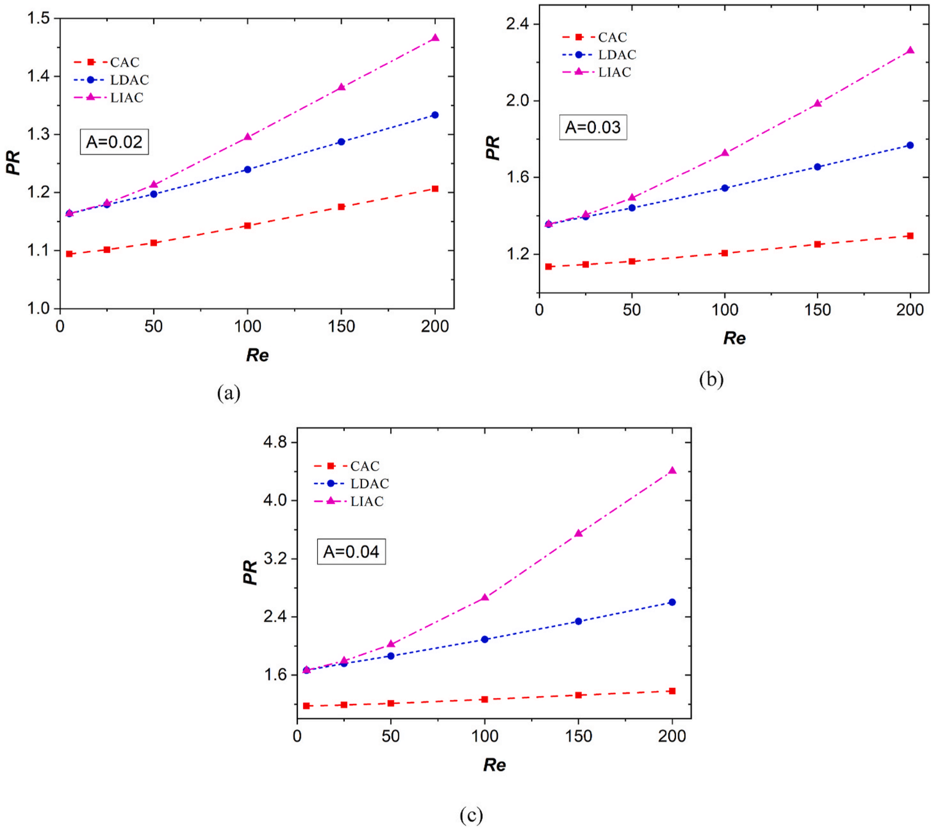

Fig. 8. Variation of *PR* for different types of wavy channels at (a) $A = 0.02$, (b) $A = 0.03$ and (c) $A = 0.04$.

values; for LDAC, $Re_{\text{crit}} = 50$ for $A = 0.02$ and $Re_{\text{crit}} = 25$ for $A = 0.03$ and 0.04; for LIAC, $Re_{\text{crit}} = 25$ at $A = 0.02$ and 0.03, and $Re_{\text{crit}} = 5$ for $A = 0.04$. For $Re < Re_{\text{crit}}$ the *PE* is the smallest for CAC and it can be even negative for $A = 0.02$, and hence CAC is not recommended for $Re < Re_{\text{crit}}$. The maximum value of *PE* is achieved for LIAC at the largest *Re* and *A* values investigated. The corresponding values at $Re = 200$ are 10.6 %, 24.0 %, and 40.3 % for $A = 0.02$, 0.03, and 0.04, respectively.

The variation of pressure drop ratio (*PR*) with *Re* is shown in Fig. 8. It is found that *PR* monotonically increases with *Re* as the pressure drop for the three channels increases with *Re* more than the pressure drop (frictional loss) for the plane channel. When comparing the *PR* values for different wavy channels we found that *PR* is the smallest for CAC irrespective of the investigated *A* values. It can be seen that the *PR* values for both LIAC and LDAC are almost the same for $Re < 25$, while for $Re > 25$, the highest value is obtained for LIAC. The main factor that determines the pressure drop ratio is the formation of recirculation zone near the outlet section (see Fig. 3). The size of recirculation zone for LIAC near the outlet is negligibly small for $Re < 25$. However, for $Re > 25$ the size is significant to increase the *PR* and as a result there is an enhancement in the difference in *PR* with LDAC for which no recirculation zone exists near the outlet due to smooth ending of wavy wall near the exit. The size of recirculation zone increases with *A* causing higher frictional losses and thus increases the *PR* value.

The heat transfer augmentation in wavy channel is usually achieved at the cost of pressure drop penalty. To study the combined effect of the pressure drop and heat transfer enhancement, the performance factor (*PF*) is analyzed to assess the needed pumping power associated with heat transfer enhancement. The variation of *PF* with *Re* is presented in Fig. 9 for different types of wavy channels and *A* values. It is found that *PF* initially decreases reaching a minimum value at a Reynolds number denoted by Re^* and increases thereafter with *Re* for all types of wavy channels and *A*, except for LIAC at $A = 0.04$. For low values of *Re* ($<Re^*$), *PR* is the dominant factor in determining the variation of *PF* in all three channels as the rate of increment in *ER* with *Re* is relatively small compared to that of *PR*. For $Re > Re^*$ the heat transfer rate is higher and thus *ER* is the dominant factor except for LIAC at $A = 0.04$ for which the value of *PR* is relatively high due to the existence of additional recirculation zones near the outlet. For lower *Re* values the highest *PF* is obtained for CAC. At higher *Re* values *PF* is the largest for LDAC at $A = 0.02$ and 0.03 and *PF* is the largest for CAC at $A = 0.04$ in the investigated *Re* domain.

5. Conclusions

In this work we investigate the thermo-hydraulic transport characteristics for forced convective flow through three types of wavy channels in the laminar regime. The flow and heat transfer rate are studied by linearly varying amplitude (*A*) and Reynolds number

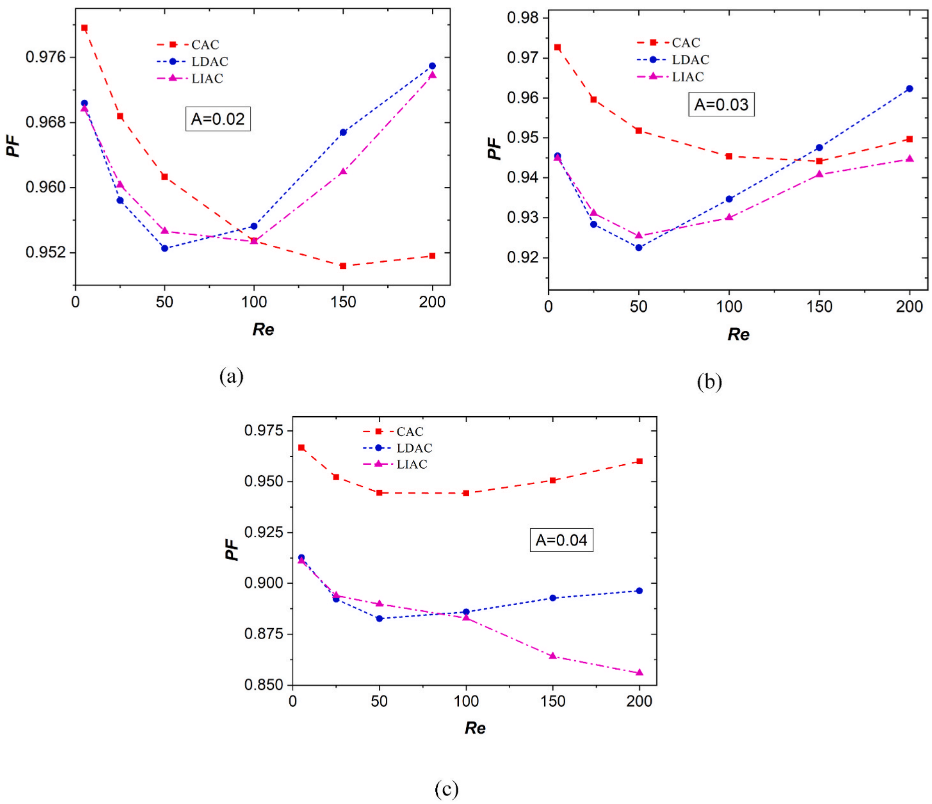

Fig. 9. Variation of *PF* with *Re* at (a) $A = 0.02$, (b) $A = 0.03$ and (c) $A = 0.04$.

(*Re*) for a linearly increasing amplitude channel (LIAC), a linearly decreasing amplitude channel (LDAC), and constant amplitude channel (CAC). The main findings are summarized as follows:

- The recirculation zones formed in the wavy passages of LIAC, LDAC and CAC play crucial role in augmenting the heat transfer as well as pressure drop. A tertiary recirculation region exists in the LIAC and LDAC at an arbitrary value of *A* in the investigated domain. For LIAC additional recirculation zones occur near the channel outlet.
- The value of average Nusselt number ($\overline{Nu}$) is almost independent on the channel geometry at low values of *Re* and *A*. At higher *Re* values, $\overline{Nu}$ is the largest for LIAC followed by LDAC and CAC. The values of percentage enhancement in heat transfer (*PE*) for LIAC at $Re = 200$ are 10.6 %, 24.0 %, and 40.3 % for $A = 0.02$, 0.03, and 0.04, respectively.
- The performance factor (*PF*) initially decreases with *Re* reaching a minimum value and increases thereafter with *Re* for all types of wavy channels and *A*, except for LIAC at $A = 0.04$. For lower *Re* values the highest *PF* is obtained for CAC. For higher values of *Re*, *PF* is the largest for LDAC at $A = 0.02$ and 0.03 and the value of *PF* is the highest for CAC in the investigated *Re* domain at $A = 0.04$.

CRediT authorship contribution statement

Sumit Kumar Mehta: Conceptualization, Numerical Simulations, Formal analysis, Writing–initial draft. **Sukumar Pati:** Conceptualization, Formal analysis, Writing - review & editing. **László Baranyi:** Conceptualization, Formal analysis, Writing - review & editing.

Declaration of competing interest

The authors declare that they have no known competing financial interests or personal relationships that could have appeared to influence the work reported in this paper.

Acknowledgments

LB acknowledges the support by the European Union and the Hungarian State, co-financed by the European Regional Development Fund in the framework of the GINOP-2.3.4-15-2016-00004 project, aimed to promote the cooperation between the higher education and the industry.

References

[1] A.A.A. Arani, A. Memarzadeh, Nanofluid multi-morphology effect on dual-fluid sinusoidal-wavy grooved absorber tube parabolic trough solar collector performances enhancement based on experimental data, Int. Commun. Heat Mass Tran. 123 (2021) 105201.
[2] D. Huu-Quan, A.M. Rostami, M.S. Rad, M. Izadi, A. Hajjar, Q. Xiong, 3D numerical investigation of turbulent forced convection in a double-pipe heat exchanger with flat inner pipe, Appl. Therm. Eng. 182 (2021) 116106.
[3] S.K. Mehta, S. Pati, Numerical study of thermo-hydraulic characteristics for forced convective flow through wavy channel at different Prandtl numbers, J. Therm. Anal. Calorim. 141 (2020) 2429–2451.
[4] S.K. Mehta, S. Pati, in: K.M. Pandey, R.D. Misra, P.K. Patowari, U.S. Dixit (Eds.), Effect of Non-uniform Heating on Forced Convective Flow through Asymmetric Wavy Channel, Recent Advances in Mechanical Engineering, Springer Singapore, 2021, pp. 333–341.
[5] S.K. Mehta, S. Pati, in: P.M. Pawar, R. Balasubramaniam, B.P. Ronge, S.B. Salunkhe, A.S. Vibhute, B. Melinamath (Eds.), Analysis of Heat Transfer and Pressure Drop for Pressure Driven Flow of Non-Newtonian Fluids through a Serpentine Channel: Influence of Prandtl Number, Techno-Societal 2020, Springer International Publishing, Cham, 2021, pp. 965–974.
[6] S.W. Chang, C.-A. Chen, Aerothermal performances of two-pass wavy ribbed channels without and with internal effusion at three bypass angles, Int. Commun. Heat Mass Tran. 128 (2021) 105614.
[7] M.P. Boruah, P.R. Randive, S. Pati, Hydrothermal performance and entropy generation analysis for mixed convective flows over a backward facing step channel with baffle, Int. J. Heat Mass Tran. 125 (2018) 525–542.
[8] M.P. Boruah, S. Pati, P.R. Randive, Implication of fluid rheology on the hydrothermal and entropy generation characteristics for mixed convective flow in a backward facing step channel with baffle, Int. J. Heat Mass Tran. 137 (2019) 138–160.
[9] D. Bhowmick, P.R. Randive, S. Pati, Implication of corrugation profile on thermo-hydraulic characteristics of Cu-water nanofluid flow through partially filled porous channel, Int. Commun. Heat Mass Tran. 125 (2021) 105329.
[10] S.K. Mehta, S. Pati, Thermo-hydraulic and entropy generation analysis for magnetohydrodynamic pressure driven flow of nanofluid through an asymmetric wavy channel, Int. J. Numer. Methods Heat Fluid Flow 31 (2021) 1190–1213.
[11] A.I. Alsabery, A. Hajjar, M.A. Sheremet, M. Ghalambaz, I. Hashim, Impact of particles tracking model of nanofluid on forced convection heat transfer within a wavy horizontal channel, Int. Commun. Heat Mass Tran. 122 (2021) 105176.
[12] Q. Xiong, A. Hajjar, B. Alshuraiaan, M. Izadi, S. Altnji, S.A. Shehzad, State-of-the-art review of nanofluids in solar collectors: a review based on the type of the dispersed nanoparticles, J. Clean. Prod. 310 (2021) 127528.
[13] M. Izadi, A. Behzadmehr, M.M. Shahmardan, Effects of inclination angle on laminar mixed convection of a nanofluid flowing through an annulus, Chem. Eng. Commun. 202 (2015) 1693–1702.
[14] M. Izadi, B. Bastani, M.A. Sheremet, Numerical simulation of thermogravitational energy transport of a hybrid nanoliquid within a porous triangular chamber using the two-phase mixture approach, Adv. Powder Technol. 31 (2020) 2493–2504.
[15] A.A. Delouei, H. Sajjadi, M. Izadi, R. Mohebbi, The simultaneous effects of nanoparticles and ultrasonic vibration on inlet turbulent flow: an experimental study, Appl. Therm. Eng. 146 (2019) 268–277.
[16] S.K. Mehta, S. Pati, in: P.M. Pawar, R. Balasubramaniam, B.P. Ronge, S.B. Salunkhe, A.S. Vibhute, B. Melinamath (Eds.), Thermo-hydraulic Performance for an Electronic Cooling System Using Porous Material, Techno-Societal 2020, Springer International Publishing, 2021, pp. 197–204.
[17] R. Mohebbi, A.A. Delouei, A. Jamali, M. Izadi, A.A. Mohamad, Pore-scale simulation of non-Newtonian power-law fluid flow and forced convection in partially porous media: thermal Lattice Boltzmann method, Phys. A: Stat. Mech. Appl. 525 (2019) 642–656.
[18] G.K. Ramesh, S.A. Shehzad, M. Izadi, Thermal Transport of hybrid liquid over thin needle with heat sink/source and Darcy–Forchheimer porous medium aspects, Arab. J. Sci. Eng. 45 (2020) 9569–9578.
[19] T.A. Rush, T.A. Newell, A.M. Jacobi, An experimental study of flow and heat transfer in sinusoidal wavy passages, Int. J. Heat Mass Tran. 42 (1999) 1541–1553.
[20] C.C. Wang, C.K. Chen, Forced convection in a wavy-wall channel, Int. J. Heat Mass Tran. 45 (2002) 2587–2595.
[21] P. Naphon, Laminar convective heat transfer and pressure drop in the corrugated channels, Int. Commun. Heat Mass Tran. 34 (2007) 62–71.
[22] P. Naphon, Heat transfer characteristics and pressure drop in channel with V corrugated upper and lower plates, Energy Convers. Manag. 48 (2007) 1516–1524.
[23] P. Naphon, Effect of corrugated plates in an in-phase arrangement on the heat transfer and flow developments, Int. J. Heat Mass Tran. 51 (2008) 3963–3971.
[24] P. Naphon, Effect of wavy plate geometry configurations on the temperature and flow distributions, Int. Commun. Heat Mass Tran. 36 (2009) 942–946.
[25] M. Akbarzadeh, S. Rashidi, J.A. Esfahani, Influences of corrugation profiles on entropy generation, heat transfer, pressure drop, and performance in a wavy channel, Appl. Therm. Eng. 116 (2017) 278–291.
[26] S. Rashidi, M. Akbarzadeh, R. Masoodi, E.M. Languri, Thermal-hydraulic and entropy generation analysis for turbulent flow inside a corrugated channel, Int. J. Heat Mass Tran. 109 (2017) 812–823.
[27] A. Saikia Shubham, A. Dalal, S. Pati, Thermo-hydraulic transport characteristics of non-Newtonian fluid flows through corrugated channels, Int. J. Therm. Sci. 129 (2018) 201–208.
[28] S. Pati, S.K. Mehta, A. Borah, Numerical investigation of thermo-hydraulic transport characteristics in wavy channels: comparison between raccoon and serpentine channels, Int. Commun. Heat Mass Tran. 88 (2017) 171–176.
[29] H. Ermagan, R. Rafee, Effect of pumping power on the thermal design of converging microchannels with superhydrophobic walls, Int. J. Therm. Sci. 132 (2018) 104–116.
[30] H. Ermagan, R. Rafee, Numerical investigation into the thermos-fluid performance of wavy microchannels with superhydrophobic walls, Int. J. Therm. Sci. 132 (2018) 578–588.
[31] M. Khoshvaght-Aliabadi, A. Jafari, O. Sartipzadeh, M. Salami, Thermal-hydraulic performance of wavy plate-fin heat exchanger using passive techniques: perforations, winglets, and nanofluids, Int. Commun. Heat Mass Tran. 78 (2016) 231–240.
[32] Y. Men, C. Liang, Z. Li, X. Tong, Configuration optimization of a membrane-based total heat exchanger with cross-corrugated triangular ducts considering thermal economy and entropy generation, Case Stud. Therm. Eng. 28 (2021) 101446.
[33] M. Jafari, M. Farhadi, K. Sedighi, Pulsating flow effects on convection heat transfer in a corrugated channel: a LBM approach, Int. Commun. Heat Mass Tran. 45 (2013) 146–154.
[34] H.A. Mohammed, A.K. Abbas, J.M. Sheriff, Influence of geometrical parameters and forced convective heat transfer in transversely corrugated circular tubes, Int. Commun. Heat Mass Tran. 44 (2013) 116–126.
[35] M.A. Ahmed, M.Z. Yusoff, N.H. Shuaib, Effects of geometrical parameters on the flow and heat transfer characteristics in trapezoidal-corrugated channel using nanofluid, Int. Commun. Heat Mass Tran. 42 (2013) 69–74.
[36] M. Jafari, M. Farhadi, K. Sedighi, Convection heat transfer of SWCNT-nanofluid in a corrugated channel under pulsating velocity profile, Int. Commun. Heat Mass Tran. 67 (2015) 137–146.
[37] H. Pehlivan, I. Taymaz, Y. Islamoğlu, Experimental study of forced convective heat transfer in a different arranged corrugated channel, Int. Commun. Heat Mass Tran. 46 (2013) 106–111.
[38] S.K. Mehta, S. Pati, Effect on non-uniform heating on heat transfer characteristics in wavy channel, in: Proceedings of the 5th International Conference on Computational Methods for Thermal Problems, 5, IISc, Bangalore, India, 2018, pp. 498–501.
[39] S.K. Mehta, S. Pati, Analysis of thermo-hydraulic performance and entropy generation characteristics for laminar flow through triangular corrugated channel, J. Therm. Anal. Calorim. 136 (2019) 49–62.
[40] E.M. Alawadhi, Forced convection flow in a wavy channel with a linearly increasing waviness at the entrance region, J. Heat Tran. 131 (2009), 011703.
[41] T.K. Nandi, H. Chattopadhyay, Numerical investigations of simultaneously developing flow in wavy microchannels under pulsating inlet flow condition, Int. Commun. Heat Mass Tran. 47 (2013) 27–31.

[42] T.K. Nandi, H. Chattopadhyay, Numerical investigations of developing flow and heat transfer in raccoon type microchannels under inlet pulsation, Int. Commun. Heat Mass Tran. 56 (2014) 37–41.
[43] N. Tiwari, M.K. Moharana, Comparative study of conjugate heat transfer in a single-phase flow in wavy and raccoon microchannels, Int. J. Numer. Methods Heat Fluid Flow 30 (2020) 3791–3825.
[44] N. Tiwari, M.K. Moharana, Numerical study of thermal enhancement in modified raccoon microchannels, Heat Tran. Res. 50 (2019) 519–543.
[45] A. Shahsavar, S.S. Alimohammadi, I.B. Askari, H.M. Ali, Numerical investigation of the effect of corrugation profile on the hydrothermal characteristics and entropy generation behavior of laminar forced convection of non-Newtonian water/CMC-CuO nanofluid flow inside a wavy channel, Int. Commun. Heat Mass Tran. 121 (2021) 105117.
[46] K. Ghachem, W. Aich, L. Kolsi, Computational analysis of hybrid nanofluid enhanced heat transfer in cross flow micro heat exchanger with rectangular wavy channels, Case Stud. Therm. Eng. 24 (2021) 100822.
[47] M.A. Ahmed, M.Z. Yusoff, K.C. Ng, N.H. Shuaib, Numerical and experimental investigations on the heat transfer enhancement in corrugated channels using SiO2–water nanofluid, Case Stud. Therm. Eng. 6 (2015) 77–92.
[48] M. Hatami, A. Kheirkhah, H. Ghanbari-Rad, D. Jing, Numerical heat transfer enhancement using different nanofluids flow through venturi and wavy tubes, Case Stud. Therm. Eng. 13 (2019) 100368.
[49] A.M. Abed, K. Sopian, H.A. Mohammed, M.A. Alghoul, M.H. Ruslan, S. Mat, A. Najah Al-Shamani, Enhance heat transfer in the channel with V-shaped wavy lower plate using liquid nanofluids, Case Stud. Therm. Eng. 5 (2015) 13–23.
[50] S.K. Mehta, S. Pati, S. Ahmed, P. Bhattacharyya, J.J. Bordoloi, Analysis of thermo-hydraulic and entropy generation characteristics for flow through ribbed-wavy channel, Int. J. Numer. Methods Heat Fluid Flow (2021), https://doi.org/10.1108/HFF-01-2021-0056.
[51] B. Farhanieh, Č. Herman, B. Sundén, Numerical and experimental analysis of laminar fluid flow and forced convection heat transfer in a grooved duct, Int. J. Heat Mass Tran. 36 (1993) 1609–1617, 1993.